Dielectric Probe: a New Electrical Diagnostic Tool for Atmospheric Pressure Non-Thermal Plasma Jet

A. Begum
Independent University, Dhaka, Bangladesh
M. Laroussi
Old Dominion University, Norfolk, VA-23529, USA
and
M. R. Pervez
Master Mind School and College, Dhaka, Bangladesh

***Abstract*—Atmospheric pressure, non-thermal plasma jet is a non-equilibrium plasma generated by electrical discharge, which is in general in room temperature. A new tool, dielectric probe is designed and used to diagnose the plasma properties of this plasma jet. To understand the jet propagation phenomenon, the plasma jet front velocity, jet current is measured by using this dielectric probe. The jet current density, reduced Electric Field (EF), and the electron density of the plasma jet along the jet axis are estimated from the current density and the jet velocity. Estimated electron density along the propagation phase of the plasma jet is in the order of 10^{11} cm^{-3} and reduced EF is around 250 Td.**

***Index Terms*—Plasma diagnostic, Plasma jet, Non-equilibrium non-thermal plasma.**

I. Introduction

Non-thermal Atmospheric Pressure Plasma Jets (NTAPPJ) are a highly non-equilibrium plasma propagating in the ambient air following the feed gas channel, outside the discharge chamber, and it is always at room temperature. In this plasma the electron temperature (T_e) is much higher than the ion/neutral temperature (T_i). Most of the developments in the plasma jet are focused on the device geometry and their applications. Teschke and his group [1] showed that the plasma jet generated by an RF power supply is a train of plasma bullets/plumes. Laroussi and Lu [2] designed the "Plasma Pencil" to generate plasma jet for bio application. This double dielectric barrier configured plasma pencil generates plasma jet of 5-8 cm long in the ambient atmosphere by using pulsed DC power supply. Lu and Laroussi [3] showed that the plasma jet is, in fact, a train of plasma bullets travelling at supersonic velocities. They used an ICCD camera to capture images of the plasma jet in the nanosecond range and found that every voltage pulse generates a plasma bullet.

The non-thermal plasma jets are widely used in bio-application [4], [5], surface decontamination [6], surface modification [7], and deposition [8]. To have better control on the plasma application it is important to understand the jet plasma properties [9]. There are many available diagnostic techniques [10]-[14] to characterize the plasma. One of the most widely used plasma diagnostic tool is Langmuir probe [15]. In Langmuir probe plasma diagnostic, a negatively and positively biased small conducting material is inserted into the discharge to collect the current. The disadvantage of the probe method are [15]-[18]: i) the plasma surrounding the probe is disturbed by the charges moving towards the probe, ii) the application of the probe is more difficult when there is oscillation or wave in the plasma, ii) probe is a direct contact method, which separate the jet plasma in perturbed and unperturbed plasma. This probe is not applicable in our case, because it entirely changes the shape and the chemistry of the small sized plasma jet. Due to the possibility of arcing Langmuir probe is also hard to place close to the outlet ($z <$ 2.0 cm) of the plasma pencil. To get the saturated probe current from which one can estimate the electron density, one has to apply a high positive bias voltage. This high bias voltage changes the plasma properties of the plasma bullets totally, and it also affects the plasma inside the discharge chamber (source of the jet plasma). The application Langmuir probe method for the estimation of the electron density of the atmospheric pressure non-thermal plasma is complicated because the collision frequency and the velocity distribution function. If there is no well-defined ground electrode, double probes are usually used in plasma diagnostics [19]. A bias voltage is applied between two probes. When this probe is placed close to the plasma jet in radial position, a fine line of plasma is created between the plasma jet and the probe, and if we place the probe into the plasma jet, all plasma is concentrated at a point on the probe. To overcome this problem, the theoreticians are working to convert the single probe data as a double probe measurement.

Manuscript received May 14, 2011.

A. Begum was with Department of Electrical and Computer Engineering, Old Dominion University, USA, now with Electrical and Computer Science Department, Independent University, Bangladesh (phone: 1-88-01753577949; e-mail: ablipi@ gmail.com or asma@secs.iub.edu.bd).

II. EXPERIMENTS

To generate the plasma jet, the plasma pencil designed by Laroussi and Lu [3] is used. This is a double dielectric barrier configured plasma pencil, where two ring electrodes are attached to two perforated dielectric disk and the disks which are separated by a 0.5 cm gap are placed in a dielectric cylinder. One of the ring electrodes is connected to the high voltage while the other is kept grounded. Helium gas flows from the high voltage end to the grounded dielectric disk, and it comes out in the ambient air through the outlet on the grounded dielectric. For the characterization of the plasma jet, a lab made probe is used to measure the jet current. This probe is made of a small copper plate covered by a dielectric sheet. The schematic of this dielectric probe is shown in Fig. 1.

The probe diagnostic method is direct contact method and there is always perturbation in the plasma due to the probe. The plasma chemistry changes due to the interaction of the plasma with the dielectric surface. To realize the change in the plasma the emission spectrum of the jet of perturbed and unperturbed plasma are collected. The main species of the helium plasma in the air are the excited nitrogen ion (391 nm), excited nitrogen (337 nm), and the metastable helium (706 nm) [20]. The arbitrary intensity of nitrogen ion, excited nitrogen and metastable helium at different position on the jet axis for perturbed and non-perturbed plasma jet are shown in Fig. 2. It doesn't show significant changes in the plasma chemistry at the interaction point of the plasma jet and the probe surface. The advantage of this probe is it can be placed close to the outlet of the plasma pencil without the possibility of arcing. The plasma has the tendency to spread over the dielectric surface. Considering this property of the plasma, the probe area is kept as small as possible, so that after reaching the probe surface the plasma jet front doesn't have enough space to spread over. The enhancement of the plasma chemistry on the probe surface is controlled in this way. The experimental set-up for the electrical diagnostic of the plasma bullet propagation along the jet axis is shown in Fig. 3. The dielectric probe is connected to the ground through a 1 kΩ resistor, and it is placed at different positions along the jet axis. As the plasma bullet/plume touches the probe, the whole system (plasma, probe, and resistor) builds a RC circuit. Compared to the time duration of the voltage pulse, the time constant (RC) of the circuit is very small so the circuit works as a differentiator and the peak current measured across the resistor is the total current of the plasma jet. A known current is applied to the probe surface and the current passing through the wire is measured to observe the response of the probe. All the measurements taken by using this probe are with a zero biased potential. In this measurement a large electron flux and a small ion flux, both are collected at the same time. As there is no external EF and the plasma bullet is an isolated plasma volume per pulse, plasma bullet and the dielectric probe always maintains a Potential Difference (PD). Because of this PD at first the electrons and then the ions accelerate towards the probe. So the first peak current in the jet current waveform is due to the electron current.

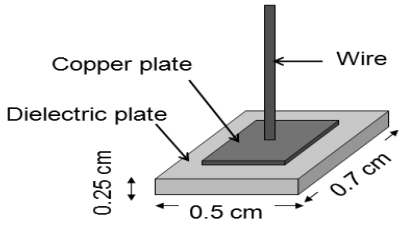

Fig. 1. Schematic of the dielectric probe.

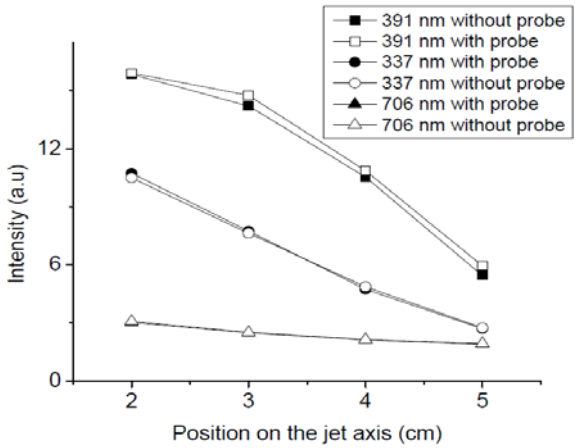

Fig. 2. The intensity of the different excited species at the perturbed and non-perturbed plasma jet.

To investigate the plasma characteristics of the plasma jet generated by the plasma pencil, Tektronix TDS784D oscilloscope, Tektronix TM502A current amplifier and current probe, and Tektronix P6015A high voltage probe are used. All the electric measurements are taken with an average of 500 acquisitions. To measure the velocity of the plasma bullet from the plasma jet current along the axis, a dielectric probe is placed at different positions starting from 1.0 cm of the jet axis and the jet current at that position is measured at that position. The plasma pencil is operated with different high voltage pulses within 5 - 7 kV range. The operating pulse widths are set within the range from 400 ns to 800 ns, and the frequency of 4 kHz. The outer hole at the grounded dielectric barrier is used as the reference position of the plasma bullet (z=0). All the results presented in this article are the average of five measurements.

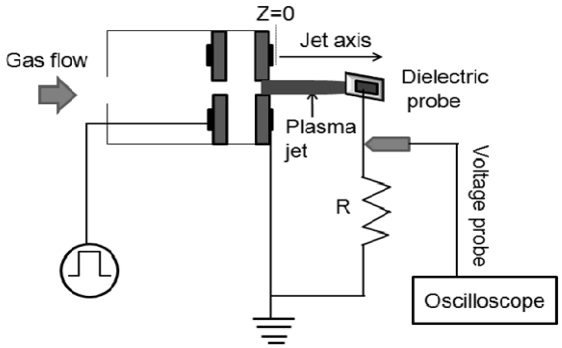

Fig. 3. Experimental set-up for the electrical investigation of the plasma bullet along the jet axis.

III. RESULTS

III.1. Velocity Measurement by Using Dielectric Probe

To understand the propagation phenomenon of the plasma jet in the ambient atmosphere, where the external electric field is negligible, the study of the plasma bullet velocity is important. The "probe" was placed at different positions along the jet axis, and the jet current was measured at those positions (Fig. 3). The jet current waveform in Fig. 4a shows that there is a time delay between the consecutive positions of the probe on the plasma bullet propagation axis. When the plasma bullet reaches the probe, the current starts to increase, reaches to its peak and from that peak value it slowly decreases with time. This current doesn't decrease to zero until the pulse is over. This is an evidence of the generation of a single bullet for every pulse and it also shows that there is a low density plasma channel behind the head of the plasma bullet. The peak current as a function of the probe's position on the jet's axis and the required time for the plasma bullet to reach that position are shown in Fig. 4b. The peak in the current curve is due to the propagation of electrons. The velocity of the plasma bullet is calculated by measuring the spatial difference between two consecutive positions of the probe and the time difference between the jet current peaks for those positions.

For three different Applied Voltages (AV) and Gas Flow Rates (GFR), plasma bullet velocities calculated in this process are shown in Fig. 5 and Fig. 6, respectively. The plasma bullet velocity curve measured by using this technique shows a similar trend as the plasma bullet velocity measured from the images of the plasma jet [21], [22]: an initial acceleration of the plasma bullet (transition phase), then a relatively constant velocity phase (propagation phase) followed by a deceleration phase. The average plasma bullet velocity at 1.0 cm on the jet axis is calculated by diving the distance of 1.0 cm with the required time for the plasma bullet to travel this distance. As the outlet of the plasma pencil is taken as the initial position of the plasma bullet, the required travel time is calculated by subtracting the formation time of the plasma bullet from the required time for the plasma bullet to reach that position (1.0 cm) on the jet axis.

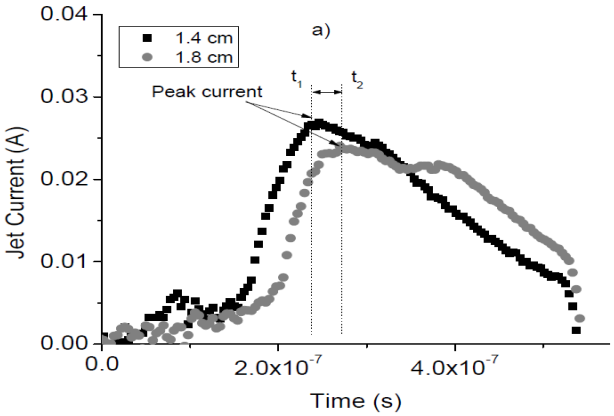

Fig. 4. a) Jet current waveform at different positions along the axis.

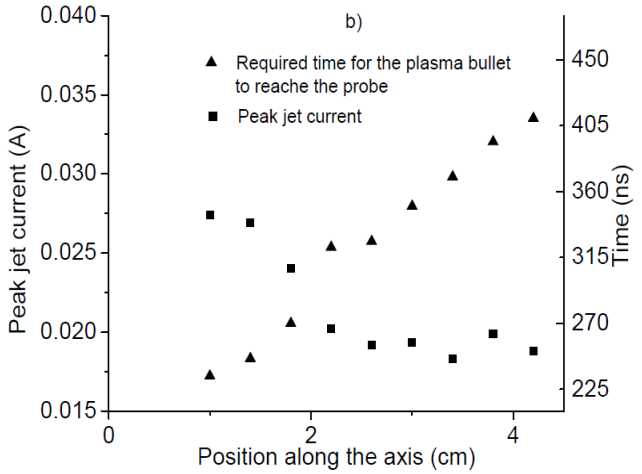

Fig. 4. b) position of the probe along the jet axis, time required for the plasma front to reach that position, and the corresponding current peaks at that position.

In Fig. 5, the plasma bullet velocity measured by using the dielectric probe for different applied voltages (5 kV, 6 kV and 6.5 kV) is shown. From its creation, velocity of the plasma bullet increases with applied voltage and reaches its peak at the end of the transition phase, which is the initial point of the propagation phase. The propagation phase of the plasma bullet starts approximately within 1.4 cm and 1.85 cm on the jet axis. The length of the propagation phase increases with applied voltage. The plasma bullet velocity along the propagation phase is higher for the longer propagation phase.

Fig. 6 shows the plasma bullet velocity for different GFRs. Similar to the velocity curve for different applied voltages, the transition phase of the plasma bullet's velocity curve ends around 1.45 cm on the jet axis. Along the propagation phase, the plasma bullet propagation velocity is higher for the feed GFR of 3.8 l/min than the propagation velocity for the GFR of 3.0 l/min and 5.8 l/min. The length of the plasma jet is highest for the gas flow rate of 3.8 l/min. It can be said that the average plasma bullet velocity is higher when the plasma bullet travels longer path. The average plasma bullet velocity also increases with applied voltage.

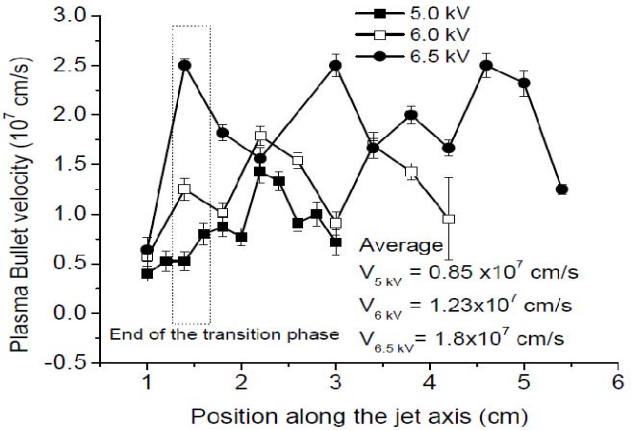

Fig. 5. Plasma bullet velocity along the jet axis for different applied voltages measured by using a dielectric probe of the operating pulse width of 500 ns and gas flow rate of 3.6 l/min.

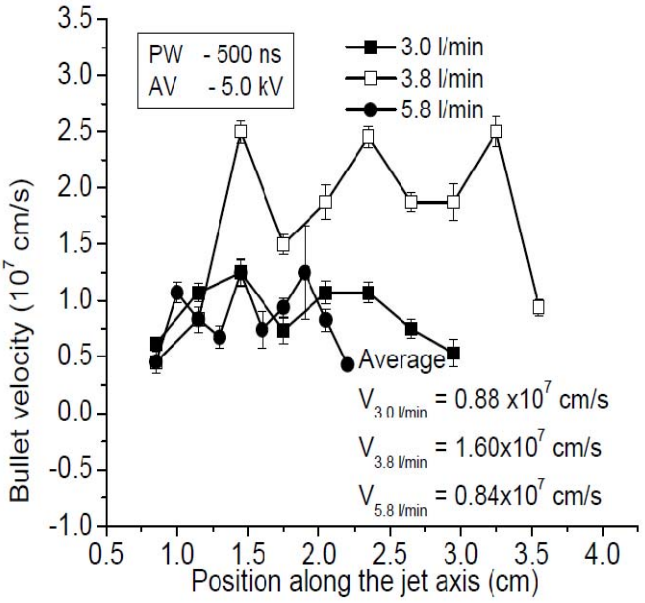

Fig. 6. Plasma bullet velocity along the jet axis for different GFRs measured by using a dielectric probe.

III.2. Electrical Characterization of the Plasma Bullet

As described in the previous section of this article, by using the dielectric probe the jet current at different positions along the jet axis can be measured. The current density is calculated from the peak jet current at a position on the jet axis and the cross-sectional area of the plasma bullet at that position. The cross section of the plasma bullet at different position on the jet axis is measured from the image of the plasma bullet. These measurements are conducted in increments of 0.4 cm from 1 cm of the axis until the end of the jet. It is shown that the jet current peak appears with delay for the different positions of the probe on the jet axis. By using a simple model *(Time delay = linear capacitance* ***x*** *linear resistance* ***x*** z^2*)* as in [23], the linear resistance (***r***) of the plasma jet for every jet segment is calculated. Here, z is the distance between the two consecutive positions of the probe. The linear capacitance of the plasma jet is calculated for a specific length of the jet assuming that it is exposed in a uniform electric field [19], [23]. It is considered that the charge is uniform along this specific segment of the plasma channel, which is only an approximation. The linear capacitance of the channel is, $c = \frac{\lambda}{U}$. Here, λ is the line charge density and *U* is the effective voltage due to the charge. The linear capacitance of the plasma jet segment is $c = \frac{2\pi\varepsilon_0}{\ln\left(\frac{d}{l}\right)}$. Where *d* is the radius of the jet, *l* is the length of the jet segment and $\varepsilon_0 = 8.54x10^{-14}$ F/cm. The estimated linear capacitance of 0.4 cm long plasma jet is 4.2 x 10^{-13} F. This linear capacitance is used in the model to calculate the linear resistance of the plasma jet. The power density (***p***) at different positions along the jet axis is calculated from the jet current by using the following equation:

$$p = \frac{4 I^2 r}{\pi D^2} \left(\frac{\mathrm{A}^2}{\mathrm{cm}^2} \frac{\Omega}{\mathrm{cm}} \right) = jE \text{ and}$$

$$\frac{p}{j} = E \left(\frac{\mathrm{V}}{\mathrm{cm}} \right) \quad (1)$$

Here, ***D*** is the diameter of the jet, ***j*** is the current density, ***r*** is the linear plasma resistance and ***E*** is the electric field due to the jet segment.

When the plasma bullet is far from the outlet of the plasma pencil, the effect of applied voltage is insignificant. From the velocity curve, it is found that the propagation phase of the plasma bullet starts around 1.45 cm of the jet axis. Consider that the applied voltage effect is insignificant and the electric field far from the bullet front is negligible when the plasma bullet propagates further than 1.4 cm of the jet axis; using Eqn. 1, the average EF of the 0.4 cm long plasma bullet is calculated.

The drift velocity of the electrons is calculated from the following equation, $v_d = \mu_e E$, here μ_e is the electron mobility. In the atmospheric pressure helium plasma, $P\mu_e$ = 0.86x10^6 cm^2.Torr/V.s [19]. This estimated electric field is not the local electric field on the plasma bullet's head. The electric field at the head of the plasma bullet is higher than the electric field in the channel behind the plasma bullet. The electron drift velocity calculated for this electric field at atmospheric pressure air ($P\mu_e$ = 0.45x10^6 cm^2.Torr/V.s) or in pure nitrogen ($P\mu_e$ = 0.42x10^6 cm^2.Torr/V.s) will be half of the calculated drift velocity in atmospheric pressure pure helium but it will be in the same order of magnitude. The average electron density in the plasma bullet (n_e) is calculated from the equation,

$$n_e = \frac{j}{e v_d} \quad (2)$$

where, j is the current density, e is the electron charge and v_d is the drift velocity of the electron. The current density and the electron density presented in the following sections are only along the propagation phase of the plasma bullet. Even the jet current is measured at 1.0 cm of the jet axis, the power density, reduced electric field and the electron density at this position are not calculated, because at 1.0 cm of the jet axis, the plasma bullet is still attached to the outlet of the plasma pencil. The jet current measurement at this position is taken to get the time delay between the current peaks at 1.0 cm and 1.4 cm of the jet axis, which is required to measure the plasma parameters at 1.4 cm of the jet axis.

Figure 7 shows the current density of the plasma bullet along the jet axis for different applied voltages. The current density increases with applied voltage. From the emergence of the plasma bullet, the current density maintains an almost steady state value/ remains constant along the propagation phase of the plasma bullet. At the end of the plasma jet, the current density increases again. It happens because the radius of the plasma bullet decreases at the end of the jet. The average reduced electric field of the plasma bullet along the

jet axis is estimated by using the Eqn. 1. The Reduced Electric Field (REF) of the plasma bullet along the jet axis is shown in Fig. 8. The reduced electric field is at maxima within 0 and 1.5 cm of the jet axis. The reduced electric field fluctuates along the propagation phase for a longer plasma jet. Otherwise it slowly decreases along the propagation phase of the plasma bullet.

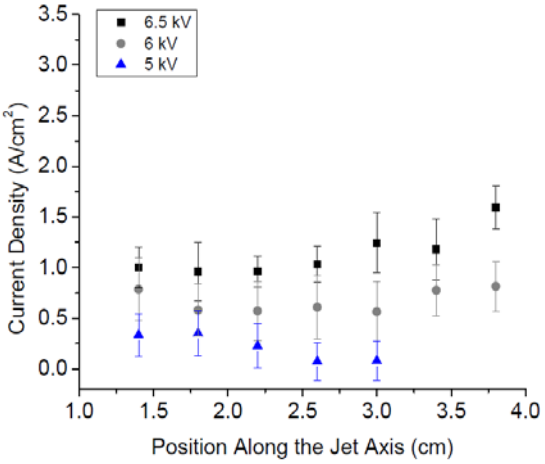

Fig. 7. Jet current density along the jet axis for three different applied voltages with the pulse width of 550 ns and feed GFR of 3.0 l/min.

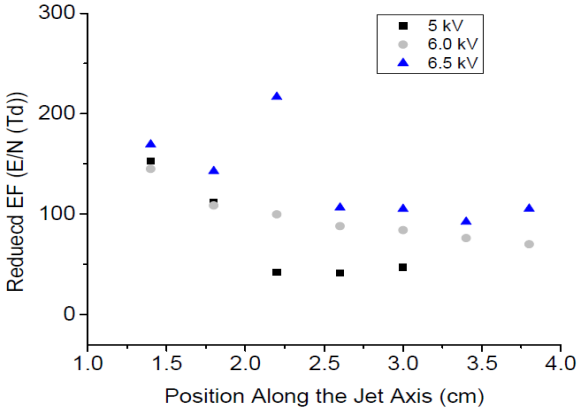

Fig. 8. Estimated average reduced electric field of 0.4 cm long plasma bullet along the jet's propagation phase.

The estimated electron density along the propagation phase is calculated from the current density and the drift velocity of the electron. This drift velocity of the electron depends on the reduced EF in the plasma. From this experimental investigation, the electron density in the plasma bullet at z < 1.4 cm is not investigated because of the difficulties to place the probe close to the outlet. For this reason, it is not possible to measure the electron density along the transition phase of the plasma bullet. The estimated electron density along the jet axis in the plasma bullet is shown in Fig. 9. It increases with applied voltage. For the applied voltage of 6 kV and 6.5 kV, the electron density reaches to its maximum value at 1.4 cm of the jet axis. There is a little fluctuation in the value of the electron density along the propagation phase of the plasma bullet. The electron density was also estimated by using the Eqn. 2 where the measured current density and the propagation velocity measured as in section III.1 were used. The estimated electron density calculated in this manner is shown in Fig. 10. The electron density is in the same order, as measured before. It also shows a fluctuation of the electron density along the propagation phase of the plasma bullet. This electron density value is higher than the estimated electron density value from the drift velocity and the current density.

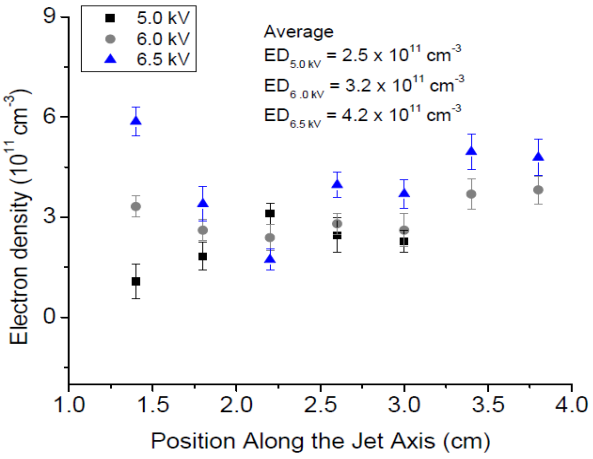

Fig. 9. Estimated Electron Density (ED) of the plasma bullet along the jet axis for different applied voltages.

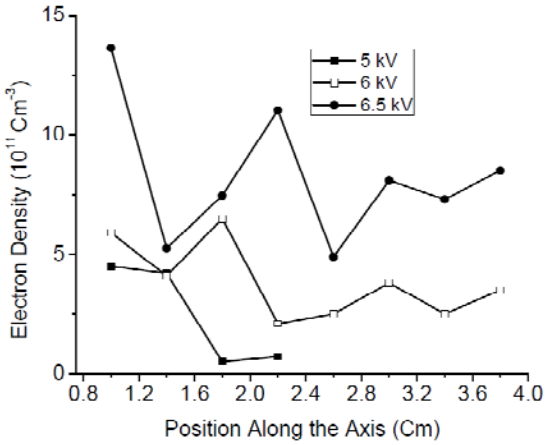

Fig. 10. Estimated Electron Density (ED) of the plasma bullet along the jet axis for different applied voltages calculated by using second method.

For short plasma jet, the fluctuation of the electron density in the plasma bullet is less. Because the drift velocity of electron in the mixture of air in helium will be lower than the calculated drift velocity, the estimated electron density will be higher than this estimated electron density in the plasma bullet. On the other hand, the average electric field is not equal to the local electric field at the tip of the plasma bullet. The local electric field is higher than the average electric field, so the drift velocity of electrons will be higher than the measured electron drift velocity. The drift velocity of the electrons in the plasma bullet is calculated from the average EF and the effect of this EF on the electrons in atmospheric pressure pure helium. This drift velocity depends on the

collision frequency of electrons with other species in the plasma. Depending on the electron drift velocity, the electron density in the plasma bullet also changes. To measure the electron density in the plasma bullet, one has to know the local electric field and the gas mixture exactly. Morrow [24] and Wu and Kunhardt [25] also observe a spatial oscillation of the electron density profile in streamer propagation in SF_6 and the mixture of N_2 - SF_6 gas, respectively. Still it does not have any well established explanation. It shows that the estimated average electron density higher when one generates a longer plasma jet. The streamer breakdown model done by Lozanskii [26] shows that at the end of the streamer, the curvature of the streamer front become sharp, and the electric field increases at the tip, which increases the electron density and the streamer front velocity. The estimated electron density measured by using the dielectric probe is in the order of 10^{11} cm^{-3}. This result is the same as the measured electron density in atmospheric pressure helium non-thermal plasma jet by using a Rogowski coil [27] and a Langmuir probe [28]. This is in one order lower than the electron density measured by microwave antenna [29].

IV. CONCLUSION AND FUTURE WORK

The characterization of the plasma bullet along the jet axis is done by using a dielectric probe. The maximum estimated average reduced electric field for the operating applied voltage of 6.5 kV and 6.0 kV is 225 Td and 150 Td, respectively. The maximum reduced electric field is at the end of the transition phase. It shows a little fluctuation of the value of electron density of the plasma bullet, which is propagating in pure helium along the jet axis. The average electron density increases with applied voltage. It is found that the estimated electron density is higher in the longer plasma jets. The plasma bullet has an inconsistent electron density value along the propagation phase, and is in order of 10^{11} cm^{-3}. At the decay phase of the streamer, the reduced electric field decreases and the gradient of the electric field at the jet front increases, so the local electron density can increase along the decay phase of the plasma jet. As the investigation of the plasma bullet by using the drift velocity and the current density of the plasma jet before 1.4 cm of the jet axis is not possible with a dielectric probe, the plasma bullet's characteristics in the transition phase is not properly understood by using a dielectric probe. The measured current density and the electron density of the plasma bullet are basically along its propagation phase. The spatial evolution of the jet electron density along the jet axis from 0.85 cm of the axis is possible when one estimate the electron density from the jet current density and the jet propagation velocity. This second method gives the higher of electron density value then the estimation using the first method. In future, work will be done to investigate the plasma jet from the beginning to the 1.4 cm of the jet axis by using dielectric probe.

REFERENCES

[1] M. Teschke, J. Kedzierski, E. G. Finantu-Dinu, D. Korzec, and J. Engemann,"High speed photograph of a dielectric barrier atmospheric pressure plasma jet," *IEEE Trans. Plasma Sci.*, vol. 33, no. 2, pp 310-311, 2005.

[2] X. Lu and M. Laroussi, " Optimization of ultraviolet emission and chemical species generation from a pulsed dielectric barrier discharge at atmospheric pressure," *J. Appl. Phys.*, vol. 98, no. 2, p 023301, 2005.

[3] X. Lu and M. Laroussi, "Dynamic of an atmospheric pressure plasma plume generated by submicrosecond voltage pulse," *J. Appl. Phys.*, vol. 100, no. 6, p 063302, 2006.

[4] E. Stoffels, I. E. Kieft, and R. E. J. Sladek, "Superficial treatment of mammalian cells using plasma needle," *J. Phys. D: Appl. Phys.*, vol. 36, no. 23, pp 2908-2913, 2003.

[5] H. W. Herrmann, I. Henins, J. Park, and G. S. Selwyn, "Decontamination of chemical and biological warfare agents using an atmospheric pressure plasma jet," *Phys. Of Plasmas*, vol. 6, no. 5, pp 2284-2289, 1999.

[6] C. Cheng, Z. Liye, R. Zhan, " Surface modification of polymer fibre by the new atmospheric pressure cold plasma," *Surface Coat. Technol*., vol. 200, no. 6659, pp 6659-6665, 2006.

[7] G. Chen, S. Chen, M. Zhou, W. Feng, W. Gu, S. Yang, The preliminary discharge characterization of a nobal APGD plume and its application in organic contaminated degradation , *Plasma Sources Sci. Technol*., vol. 15, no. 603, pp 603-608, 2006.

[8] H. Ha, B. K. Moon, T. Horiuchi, T. Inushima, H. Ishiwara, and H. Koinuma, "Structure and electric properties of TiO_2 films prepared by cold plasma torch under atmospheric pressure" *Mater. Sci. Eng.,* vol. B41, no. 1, pp 143-147, 1996.

[9] D. B. Kim, J. K. Rhee, S. Y. Moon, and W. Choe, "Study of geometrical and operational parameters cotrolling the low frequency microjet atmospheric pressure plasma characteristics," *Appl. Phys. Lett*., vol. 89, no. 6, pp 061502-0615024, 2006.

[10] R. L. Hickok, "A survey of plasma diagnostic technique," *IEEE transaction on nuclear science*, vol. 28, no. 17, 1981.

[11] G. Bockle, J. Ehrhardt, P. Kirschesch, N. Wenzel, R. Batzner, H. Hinsch, and K. Hubner, "Spatially resolved light scattering diagnostic of plasma focused devices," *Plasma Physics and control fusion*, vol. 34, no. 5, pp 801-841, 1992.

[12] B. H. Kolner, P. M. Conklin, R. A. Buckles, N. K. Fontain, and R. P. Scott, "Time resolved pulsed-plasma characterization using broad band terahertz pulses correlated with fluorescence imaging," *Appl. phys. Lett.,* vol. 87, no. 15, pp 151501-151503, 2005.

[13] J. Liu and X.-C. Zhang, "Plasma characterization using terahertz-wave-enhanced fluorescence," *Applied phys. Let.* Vol 96, no 4, p 041505, 2010.

[14] V. Motto-Ros, M. Boueri, W. Lei, Ma. Qianli, L. zheng, H. zeng, and J. Yu, "Time- and Space- resolved emission spectroscopy of laser-induced plasma and its application for trace element detection," *Laser and Electro optic & the pacific rim conference on laser and electro optics,* Aug. 2009..

[15] R. F. Eckman, "Langmuir probe measurement in the plume of pulsed plasma" M.Sc thesis, Department of Mechanical Engineering, Worcester Polytechnic Institute, USA.

[16] M. A. Razzak, S. Takamura, S. Saito, and M. R. Talukder, "Estimation of plasma parameters for microwave-sustained Ar/He plasma at atmospheric pressure," *Contrib.Plasma Phys.*, vol. 50, no. 9, pp 871-877, 2010.

[17] Michael T. C. Fang, J. L. Zhang, and J. W.Yan, "On the use of Langmuir probes for the diagnosis of atmospheric thermal plasmas," *IEEE Tans. On Plasma Sci.*, vol. 33, no. 4, pp 1431-1442, 2005.

[18] D. R. Boris, R. F. Frensler, and S. G. Walton, "The LC resonance probe for determining local plasma density," *Plasma source Sci. and technology*, vol. 20, pp 25003-25010, 2011.

[19] Y. P. Reizer, *Gas Discharge Physics*, Springer-verlag, 1991.

[20] N. Mericam-Bourdet, M. Laroussi, A. Begum, and E. Karakas, "Experimental investigation of plasma bullet," *J. Phys. D: Appl. Phys.*, vol. **42**, no. 5, p 055207, 2009.

[21] A. Begum, E. Karakas, "Investigation of plasma bullet velocity by electrical and optical technique", *International Conference on Plasma Science, ICOPS 2010, Norfolk, VA*.
[22] A. Begum, M. Laroussi, "Electrical characterization of plasma jet", *International Conference on Plasma Science, ICOPS 2010, Norfolk, VA.*
[23] E. M. Bazelian, and Y. P. Reizer, *Spark Discharge,* 1st Ed. CRC-Press, 1998.
[24] R. Morrow, *Phys. Rev. A-Gen.Phys*., "Properties of streamers and streamer channels in $SF_{6,}$" vol. 35, no. 4, pp 1778-1785, 1987.
[25] C. Wu and E. E. Kundhardt, "Formation and propagation of streamer in N_2 and N_2-SF_6 mixtures," *Phys. Rev. A-Gen. Phys.* , Vol. 37, no. 11, pp 4396-4406, 1988.
[26] E. D. Lozanskii, *Sov. Phys-Uspekhi*, "Developments of electron avalanches and streamers," vol. 18, no. 11, pp 893-908, 1975.
[27] A. Shashnurin, M. N. Shneider, A. Dogariu, R. B. Miles, and M. Keidar, "Temporal behavior of cold atmospheric plasma jet," *Appl. Phys. Lett.*, vol. 94, no. 23, p 231504, 2009.
[28] O. Sakai, Y. Kishimoto, and K. Tachibana, *J. Phys. D: Appl. Phys.*," Integrated coaxial-hollow micro-dielectric barrier-discharges for a large–area plasma source operating at around atmospheric pressure," vol. 38, no. 3, p 431, 2005.
[29] A. Shashnurin, M. N. Shneider, A. Dogariu, R. B. Miles, and M. Keidar, "Temporary- resolved measurement of electron density in small atmospheric plasmas," *Appl. Phys. Lett.*, vol. 96, no. 171502, 2009.